



The Light-to-Nutrient Ratio in Alpine Lakes: Different Scenarios of Bacterial Nutrient Limitation and Community Structure in Lakes Above and Below the Treeline

Yaling Su¹ · Yingxun Du¹ · Peng Xing¹

Received: 9 May 2021 / Accepted: 28 July 2021 / Published online: 7 August 2021

© The Author(s), under exclusive licence to Springer Science+Business Media, LLC, part of Springer Nature 2021

Abstract

The light-to-nutrient hypothesis proposes that under high light-to-nutrient conditions, bacteria tend to be limited by phosphorus (P), while under relatively low light-to-nutrient conditions, bacteria are likely driven towards carbon (C) limitation. Exploring whether this light-to-nutrient hypothesis is fitting for alpine lakes has profound implications for predicting the impacts of climatic and environmental changes on the structures and processes of aquatic ecosystems in climate-sensitive regions. We investigated the environmental conditions and bacterioplankton community compositions of 15 high-elevation lakes (7 above and 8 below treeline). High light-to-nutrient conditions (denoted by the reciprocal value of the attenuation coefficient ($1/K$) to total phosphorus (TP)), high chlorophyll *a* (Chl *a*) concentrations, low TP concentrations and low ratios of the dissolved organic carbon concentration to the dissolved total nitrogen concentration (DOC:DTN) were detected in above-treeline lakes. Significant positive correlations between the bacterioplankton community compositions with $1/K$:TP ratios and Chl *a* concentrations indicated that not only high light energy but also nutrient competition between phytoplankton and bacteria could induce P limitation for bacteria. In contrast, low light-to-nutrient conditions and high allochthonous DOC input in below-treeline lakes lessen P limitation and C limitation. The most abundant genus, *Polynucleobacter*, was significantly enriched, and more diverse oligotypes of *Polynucleobacter* operational taxonomic units were identified in the below-treeline lakes, indicating the divergence of niche adaptations among *Polynucleobacter* oligotypes. The discrepancies in the light-to-P ratio and the components of organic matter between the above-treeline and below-treeline lakes have important implications for the nutrient limitation of bacterioplankton and their community compositions.

Keywords Bacterioplankton · Alpine lakes · Light-to-nutrient hypothesis · *Polynucleobacter* · Oligotypes · Niche separation

Introduction

The amount of solar energy and the amount of nutrients (such as nitrogen and phosphorus) are two major factors that determine the structures and processes of aquatic ecosystems. Solar radiation is the main energy source for aquatic ecosystems, and photosynthetically active radiation (PAR) from the 400–700-nm wavelengths of visible light plays a decisive role in the growth of various organisms and the

primary production of lakes. Moreover, the photochemical degradation of dissolved organic carbon (DOC) profoundly affects the underwater light intensities and carbon cycles in lakes. In addition, large-scale fertilizer use in the last two decades has greatly increased the input and accumulation of nutrients in freshwater ecosystems [1]. The light-to-nutrient hypothesis indicates that the balance between light and nutrients manipulates the ‘nutrient use efficiency’ in lacustrine food webs [2] and that under high light-to-nutrient conditions, bacteria tend to be limited by phosphorus (P) because high light energy and low nutrient availability decrease phytoplankton biomass production and promote the exudation of labile carbon (C), which can be easily utilized by bacteria [3]. In contrast, under relatively low light-to-nutrient conditions, relatively abundant P increases phytoplankton biomass production and reduces the exudation of labile C. Bacteria

✉ Peng Xing
pxing@niglas.ac.cn

¹ State Key Laboratory of Lake Science and Environment, Nanjing Institute of Geography and Limnology, Chinese Academy of Sciences, No. 73 East Beijing Road, Nanjing 210008, China

might therefore be driven towards C limitation under these conditions. Chrzanowski and Grover compared the frequencies of P and C limitations in two lakes and provided evidence supporting the light-to-nutrient hypothesis [4].

In general, the light-to-nutrient hypothesis is based on the idea that bacteria live mainly on the organic C produced by phytoplankton. However, Sterner et al. [2] pointed out that there are limits to this hypothesis. For example, in some ecosystems where DOC cycling is governed by allochthonous inputs, the light-to-nutrient hypothesis might be modified. Dissolved organic carbon from allochthonous origin can also maintain the growth of bacterioplankton, which might decouple the tight connection between bacterioplankton and the primary production [5, 6]. To date, studies on whether such aquatic ecosystems with abundant allochthonous C fit the above interpretation and the mechanism behind it are lacking.

Remote polar, subpolar and alpine lakes are extremely sensitive to climate warming and have fundamentally different physical structures from those of lowland lakes. The former are primarily fed by runoff from melted ice and snow as well as atmospheric precipitation; thus, large quantities of allochthonous C are transferred to these alpine lakes. With climate warming, it is estimated that ~48 Tg of DOC stored in the world's glaciers and ice sheets will be released in glacial runoff by 2050 [7]. Moreover, atmospheric depositions of nutrients caused by human activities have significant impacts on the ecosystems in these remote lakes [8]. In North America, the atmospheric deposition of reactive nitrogen has changed alpine lakes from nitrogen-limited conditions to nitrogen-saturated conditions [9], thereby changing the nutrient limitation conditions of these lakes from the previous nitrogen limitation to phosphorus limitation [10]. One important consequence of climate warming and increased nutrient loadings is that treelines are rising in high-elevation and high-latitude regions, and the vegetation cover above the treeline is increasing along with lake primary production [11]. Therefore, exploring whether alpine lakes with abundant allochthonous C fit the light-to-nutrient hypothesis has profound implications for predicting the impacts of future climatic and environmental changes on the structures and processes of the aquatic ecosystems in these regions.

Polar and high-elevation lakes are generally oligotrophic and P-limited [12]. In addition, higher solar radiation levels in high-elevation regions lead to higher light:P ratios in alpine lake waters than in low-land lake waters. Theoretically, bacteria tend to be limited by P under such high light-to-nutrient conditions; however, little information is available on the actual responses of bacteria to light-to-nutrient conditions in different types of high-elevation lakes. For example, high-elevation lakes include those located above and below treelines. The concentrations of DOC and P in below-treeline lakes are significantly higher than those in

above-treeline lakes, but the solar radiation level shows the reverse trend [12, 13]. Moreover, the chromophoric dissolved organic matter (cDOM) fluorescence in above-treeline lakes is predominantly contributed by protein-like components, whereas that in below-treeline lakes is mainly contributed by terrestrial humic-like components [12]. These discrepancies in the light and nutrient conditions and the compositions of organic matter between above-treeline and below-treeline lakes may have important implications for bacterial growth and community structures, thereby affecting the responses of bacteria to various light-to-nutrient conditions.

We found that the ecosystems in alpine lakes had different properties in different mountain environments during our investigation of solar radiation and nutrient levels in above-treeline and below-treeline alpine lakes. Above-treeline lakes are mainly surrounded by exposed rocks and alpine meadows, while forests encircle below-treeline lakes. The studied lakes also showed significant differences in their light and nutrient levels [12]. In this work, we collected data on the solar light intensity, nutrient level, cDOM composition, bacterial abundance and community composition in fifteen alpine lakes to test whether bacterial nutrient limitation conditions in alpine lakes fit the light-to-nutrient hypothesis and to investigate whether bacterial community compositions and functions are affected by the light-to-nutrient ratio. We used the attenuation coefficient (K) rather than instantaneous irradiance because the former is appropriate for comparing underwater optical characteristics among different lakes, minimizing the impacts of the weather changes that occurred during the sampling periods. Specifically, we hypothesized that bacteria are P limited in above-treeline lakes but not C limited in the below-treeline lakes and that bacterial community composition is influenced by light-to-nutrient conditions.

Materials and Methods

Study Sites and Sampling

We investigated fifteen alpine lakes in Yunnan Province, Southwest China (Table S1, Supporting Information). Among these lakes, seven were located above the treeline on Haba Snow Mountain (27°10'–27°24'N, 100°02'–100°14'E), with elevations of ~4200 m above sea level (Fig. S1a, Supporting Information), and eight were located below the treeline on Yunnan Laojun Mountain (26°38'–27°15'N, 99°07'–100°00'E), with elevations ranging from 3800 to 3900 m (Fig. S1b, Supporting Information). Each studied lake had a small surface area (<5 km²) and was mainly fed by precipitation and seasonal streams. The sampling work was performed in September of 2013. The water depth of

each lake was determined using an ultrasonic depth finder. Water was sampled using a 5-L Niskin water sampler and kept in 5-L acid-washed polypropylene plastic bottles under ice for further filtration and measurement. The cDOM samples were obtained from the lake water by filtration over a 0.22- μm Millipore membrane cellulose filter. The filtered water was divided into two parts: one part was used for the cDOM sample analysis, and the other was used for the bacterial abundance estimation. The cDOM samples were collected in brown glass bottles and brought back to the laboratory under ice. The bacterial samples were simultaneously collected into 5-mL sterilized bottles, followed by the addition of formalin (2% final concentration) to determine the bacterial abundance counts.

Water Quality Parameters and Attenuation Coefficient

We measured the water temperatures using a multi-parameter water quality measuring instrument (YSI 556 MPS). The total nitrogen (TN) and total phosphorus (TP) concentrations were analysed using a spectrophotometer (Shimadzu UV2401 UV-Vis) by alkaline potassium persulphate digestion and the molybdenum blue method, respectively. The water samples were filtered with Whatman GF/C filters and then extracted with ethanol to obtain the chlorophyll *a* (Chl *a*) sample. The concentration of Chl *a* was determined with a spectrophotometer at 750 nm and 665 nm. To determine the DOC concentration, the lake water was filtered over a 0.22- μm Millipore membrane; then, the DOC was measured using a high-temperature static pressure concentration analysis method.

The instantaneous irradiation intensity was recorded using a RAMSES-ACC-UV-VIS hyperspectral radiometer (Fig. S2, Supporting Information); however, these measurements were strongly influenced by the weather conditions. Therefore, the attenuation coefficient (*K*) was estimated through exponential regressions of the photosynthetically active radiation intensity at different depths to compare the underwater optical characteristics among different lakes. The general water quality parameters of each studied lake are presented in the Supporting Information Table S1. We examined the significances of the measured differences in the above parameters among lakes using a *t* test for independent samples and a *p* value of 0.05.

cDOM Optical Measurements and Parallel Factor Analysis (PARAFAC)

The cDOM fluorescence excitation-emission matrices (EEMs) were measured in a quartz cuvette (light path = 0.01 m) on a Hitachi F-7000 fluorescence spectrometer (Hitachi High-Technologies, Japan) equipped with a

700-voltage xenon lamp. The excitation wavelengths ranged from 200 to 450 nm at increments of 5 nm, and the emission wavelengths ranged from 250 to 600 nm at increments of 2 nm. Instrumental corrections were performed according to the procedure recommended by the Hitachi F-7000 Instruction Manual [13]. Several post-acquisition steps were carried out to correct and standardize the measured data: (i) the inner filter effect was corrected using the absorption spectra [14]; (ii) a blank correction was conducted by subtracting the EEM spectra of Milli-Q water; and (iii) the data were normalized relative to the area of the Raman peak of Milli-Q water. The corrected fluorescence spectra were used for the parallel factor analysis (PARAFAC) model. PARAFAC is used to reduce matrix data into discrete components that represent DOM pools of different sources or compositional characters. A PARAFAC analysis was carried out following standard procedures [15] using the DOMFluor toolbox in MATLAB (R2017a, Mathworks). Prior to the PARAFAC analysis, the corrected EEM wavelength ranges were reduced to 250–450 nm for excitation and 280–500 nm for emission, and the Rayleigh scatter was removed. Fifty-four samples were used to create the PARAFAC model, including 24 samples obtained in this study and 30 other samples obtained during the same sampling time in the study area. A four-component model (C1–C4) was validated using a split-half analysis and random initialization [15]. The model generated the fluorescent intensity (R.U.) of each component in each sample. FI370 ($\lambda_{\text{Ex}} = 370 \text{ nm}$, F470/F520) is a useful index that represents the relative contributions of aromatic amino acids and non-aromatic substances to the fluorescence intensity [16]. Thus, it has been used as a tracer of the source and degradation degree of cDOM.

Bacterial Abundance Measurements

All samples were filtered through a 0.22- μm black polycarbonate membrane and then stained with 4'-diamidino-2-phenylindole for 20 min in the dark [17]. Enumeration was performed visually using a Zeiss fluorescence microscope (AxioCam-MRC-5). We counted over 20 duplicate fields per slide.

DNA Extraction, Sequencing and Data Analysis

Microbial DNA was extracted from the filters using an E.Z.N.A.® Water DNA Kit (Omega Biotek, Norcross, GA, USA) according to the manufacturer's protocols. The primers 515F (5'-GTGCCAGCMGCCGCGG-3') and 907R (5'-CCGTCAATTCMTTTRAGTTT-3'), targeting the V4–V5 hypervariable regions of bacterial 16S rRNA genes, were selected for PCR amplification [18]. PCR products from different samples were sequenced on a MiSeq platform (Illumina, Inc., San Diego, CA, USA) using a 2 \times 250-paired-end

sequencing kit at Shanghai BIOZERON Biotechnology Co., Ltd. (Shanghai, China).

Trimmomatic software was used to process the raw sequence data for quality control [19]. The PE reads were overlapped to assemble the final tag sequences with a minimum overlap length of 10 bp. We removed all sequences that contained more than one ambiguous base ‘N,’ those that contained any errors in the forward or reverse primers and those with mismatch ratios greater than 0.2 within the overlap region. The tail bases of reads with quality values below 20 were filtered, and variable tags (overlap lengths minus primers and barcodes) that were shorter than 50 bp were also removed. The obtained clean sequences were then analysed using QIIME software [20]. The clean sequences were screened for chimeras using Usearch [21]. To correct for differences in the sequencing depths, 18,997 sequences of each sample were sub-sampled randomly for the downstream analysis. Sequences with similarities > 97% were clustered into one operational taxonomic unit (OTU) using the UCLUST algorithm [22]. In total, 2648 OTUs were generated throughout the 24 samples. A representative sequence of each phylotype was aligned using PyNAST [20] with a relaxed neighbour-joining tree built using FastTree [23]. The taxonomic assignments of the OTU-representative sequences were performed against the SILVA database (release_128) [24] at 80% similarity using the RDP Classifier [25].

The alpha diversity, reflected by the species richness (SR, i.e. the number of OTUs), and Pielou’s evenness were calculated using the vegan package version 2.2–1 in R 3.1.2. Faith’s phylogenetic diversity (Faith’s PD) was measured using the phylogenetic tree and the OTU table with the pd command in the picante package in R. The beta diversity, which reflects the differentiation of bacterial community compositions among habitats in a landscape, was measured using the Bray–Curtis distances with the R function “vegdist” (method = “bray”; package “vegan”).

Oligotyping Analysis of the Dominant OTUs

The intra-OTU micro-diversities of the representative OTUs were analysed by oligotyping, which facilitated the detection of single-nucleotide variations by excluding sequencing error effects based on the Shannon entropy values [26]. Considering that rare OTUs would not provide sufficient oligotype information and to minimize the impact of sequencing errors on the oligotyping results, OTUs that were present in fewer than 50% of samples within each group or those with less than 0.01% abundance in all sequences were discarded from further analysis. Oligotyping was performed by using the oligotyping pipeline version 2.1, available at <https://github.com/merenlab/oligotyping>. After the first step involving the sequence alignment and entropy figure generation, the number of components (-c parameter) was

identified manually in the analyse-entropy script within the oligotyping pipeline. The minimum substantive abundance parameter (-M parameter) was always set to 10.

Statistical Analysis

Test of Significance

The significant differences in environmental factors and species richness between the lakes above and below the treelines were assessed by one-way analysis of variance (ANOVA) and Tukey’s HSD post hoc comparison using SPSS 19.0 software. We further evaluated the significances of the compositional differences between the two regions using the permutational multivariate analysis of variance (PERMANOVA) method based on Bray–Curtis dissimilarity with 999 permutations. This analysis was performed using the “vegan” package in R.

To identify the phyla or genera whose relative frequencies (rel. freq. %) in the above-treeline communities differed significantly from those in the below-treeline samples, a two-sided Welch’s *t* test (*p* value) was used in STAMP v2.01 software [27].

Multivariate Statistical Analysis

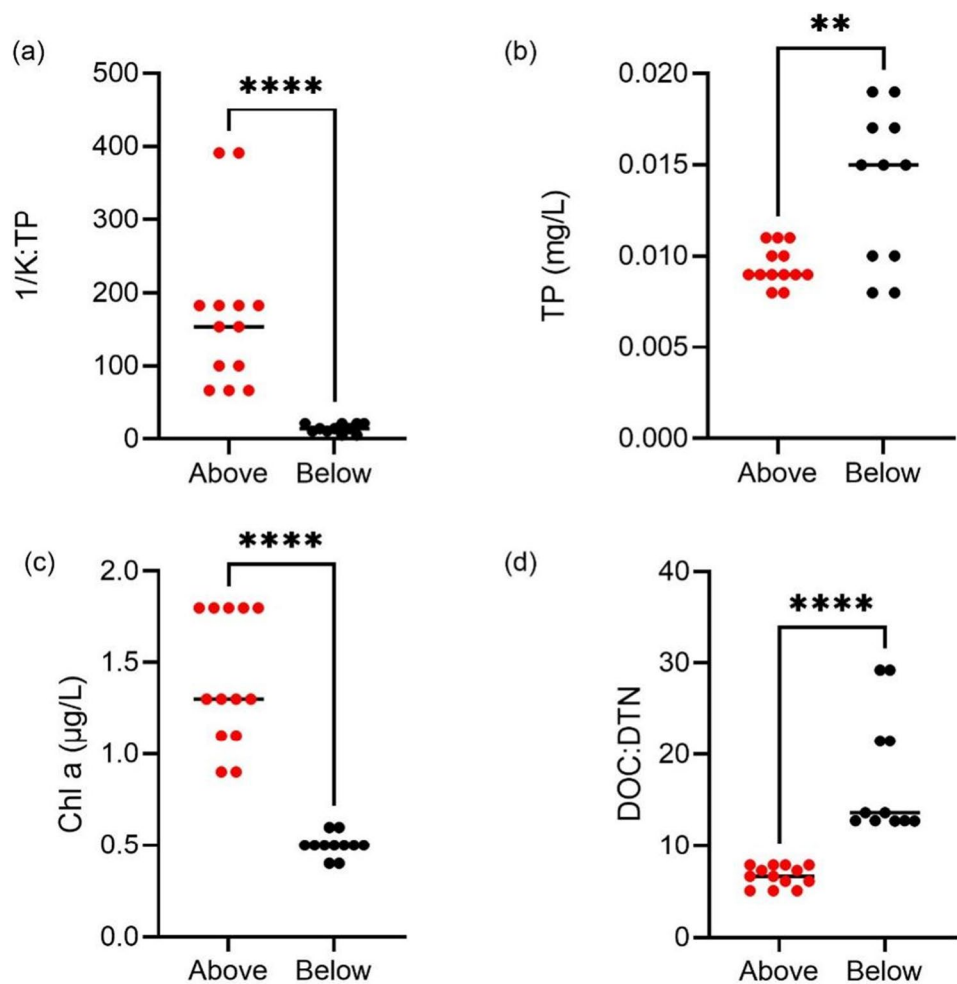
A redundancy analysis (RDA) was performed to detect the relationships between the bacterial community composition and explanatory variables because the length of the first detrended correspondence analysis (DCA) axis run on the species data was < 2. Ten environmental variables (1/K:TP, Temp, pH, DOC:TN, TP, Chl *a*, C2–C4 fluorescent components and FI370) were included in the analysis. We used forward selection to note the significant factors that shaped the bacterial community composition by 1000 simulated permutations (*p* < 0.05). A RDA was performed using the program CANOCO 5.0 [28], and a significance test was carried out by Monte Carlo permutation (999 times). Niche separations within dominant OTUs were detected using a RDA of the oligotype distributions along with the explanatory variables.

Results

Light-to-Nutrient Ratio in Alpine Lakes

In this work, a high reciprocal value of the attenuation coefficient (1/*K*) corresponded to high underwater light energy. Therefore, a high 1/*K*:TP ratio indicated a high light:TP ratio. The 1/*K*:TP ratios in the above-treeline lakes (mean value: 170.9) were significantly higher than those in the below-treeline lakes (mean value: 14.6) (Fig. 1, *p* < 0.001). The TP concentrations in the above-treeline lakes (mean

Fig. 1 Comparison of the 1/K:TP ratios (a), TP concentrations (b), Chl *a* concentrations (c) and DOC:DTN ratios (d) in the above-treeline and below-treeline lakes. *K* represents the light attenuation coefficient (m^{-1}). **** $p < 0.0001$; ** $p < 0.01$



value: $8 \mu\text{g/L}$) were significantly lower than those in the below-treeline lakes (mean value: $13 \mu\text{g/L}$) (Table S1, $p < 0.001$). Moreover, the attenuation coefficients (mean value: 0.8 m^{-1}) were remarkably lower in the above-treeline lakes than those in the below-treeline lakes (mean value: 5.7 m^{-1}) (Table S1, $p < 0.001$), indicating much weaker underwater light intensities and lower light:TP ratios in the below-treeline lakes than the corresponding above-treeline values. Therefore, the high 1/K:TP ratios measured in the above-treeline lakes were attributed to both high 1/K values and low TP concentrations. The lower underwater light intensities obtained in the below-treeline lakes resulted from the large amounts of humus inputs. It is interesting to note that the concentrations of Chl *a* in the above-treeline lakes were obviously higher than those in the below-treeline lakes. Since Chl *a* concentrations are usually highly correlated with phytoplankton abundance or biomass [29], the relatively high Chl *a* concentrations measured in the above-treeline lakes ($1.4 \mu\text{g/L}$) compared to those in the below-treeline lakes ($0.5 \mu\text{g/L}$) indicated higher phytoplankton abundances despite lower TP concentrations in the former lakes. In addition, the DOC:DTN ratios in the above-treeline lakes (3.0)

were significantly lower than those in the below-treeline lakes (14.0) ($p < 0.001$).

The bacterial abundances in the above-treeline lakes (mean value: 26,118 cells/mL) were lower than those in the below-treeline lakes (mean value: 33,151 cells/mL) (Table 1). We further performed a linear regression of the natural logarithm of the bacterial abundances, the $\log(1/K:TP)$ values and the Chl *a* concentrations (Fig. 2). In the above-treeline lakes, the $\log(\text{bacterial abundance})$ presented a positive correlation with the $\log(1/K:TP)$ values ($R^2 = 0.72$, $p < 0.05$) and a negative correlation with the Chl *a* concentrations ($R^2 = 0.62$, $p < 0.05$). In the below-treeline lakes, the $\log(\text{bacterial abundance})$ showed little correlation with either the $\log(1/K:TP)$ values ($R^2 = 0.11$) or the Chl *a* concentrations ($R^2 = 0.0005$).

cDOM Components

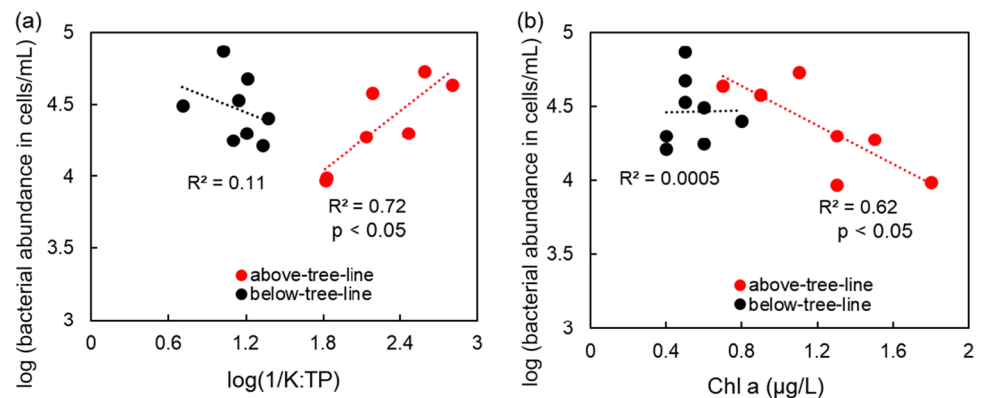
A PARAFAC model consisting of four fluorescent components was developed to analyse the cDOM in the studied lakes (Fig. 3). Component 1 (C1) (emission maximum of 442 nm with 325- and < 250 -nm excitations) was categorized

Table 1 One-way ANOVA of major physiochemical factors between lakes above and below the tree line

| Factors | Above tree line | | Below tree line | | <i>F</i> | <i>p</i> |
|-----------------------------|-----------------|-------|-----------------|--------|----------|----------|
| | Average | Std | Average | Std | | |
| <i>K</i> (m ⁻¹) | 0.84 | 0.41 | 6.06 | 2.17 | 72.736 | *** |
| Temperature (°C) | 7.41 | 2.28 | 9.28 | 1.82 | 4.801 | * |
| Conductivity (mS/cm) | 0.08 | 0.02 | 4.57 | 6.61 | 6.055 | * |
| pH | 8.43 | 0.33 | 7.72 | 0.34 | 27.262 | *** |
| DO (mg/L) | 14.35 | 20.72 | 7.12 | 0.96 | 1.326 | ns |
| DOC (mg/L) | 1.99 | 0.34 | 5.67 | 1.65 | 45.145 | *** |
| TN (mg/L) | 0.72 | 0.19 | 0.61 | 0.32 | 1.058 | ns |
| DTN (mg/L) | 0.30 | 0.05 | 0.33 | 0.02 | 2.110 | ns |
| NH ₄ -N (mg/L) | 0.07 | 0.04 | 0.10 | 0.04 | 1.668 | ns |
| NO ₃ -N (mg/L) | 0.18 | 0.04 | 0.15 | 0.05 | 4.636 | * |
| NO ₂ -N (μg/L) | 1.23 | 0.44 | 1.37 | 0.61 | 1.304 | ns |
| TP (μg/L) | 9.46 | 1.05 | 13.91 | 4.18 | 13.782 | ** |
| DTP (μg/L) | 8.01 | 1.15 | 9.75 | 1.58 | 9.729 | ** |
| PO ₄ -P (μg/L) | 3.37 | 0.11 | 4.91 | 0.65 | 76.882 | *** |
| Chl <i>a</i> (μg/L) | 1.40 | 0.36 | 0.50 | 0.06 | 68.063 | **** |
| Comp1 | 0.15 | 0.14 | 1.09 | 0.50 | 42.726 | *** |
| Comp2 | 0.08 | 0.14 | 0.67 | 1.00 | 3.496 | ns |
| Comp3 | 0.29 | 0.34 | 0.11 | 0.12 | 2.739 | * |
| Comp4 | 0.04 | 0.04 | 0.14 | 0.08 | 15.288 | ns |
| Bacterial species richness | 474.85 | 73.89 | 559.18 | 194.14 | 2.107 | ns |

ns not significant

*** $p < 0.001$; ** $p < 0.01$; * $p < 0.05$

Fig. 2 Linear correlation of the natural logarithm of the bacterial abundance (cells/mL) with the $\log(1/K:TP)$ (a) and of the $\log(\text{bacterial abundance})$ with the Chl *a* concentrations (μg/L) (b) in the above-treeline and below-treeline lakes

as a mixture of traditional humic-like peaks A and C [30], which were traditionally termed terrestrial humic-like components [31–33]. Component 2 (C2, excitation/emission $\leq 250/300$, 340 nm) and Component 3 (C3, excitation/emission = 270/302 nm) were identified as proteinous materials corresponding to tyrosine-like and tryptophan-like components, respectively [33–36]. Component 4 (C4, excitation/emission $\leq 250/295$, 400 nm) corresponded to what is termed the ‘M’ peak; this component represents humic substances and has been described as the products resulting from microbial processes or autochthonous production [31, 36].

The overall cDOM components were significantly different between the samples collected from the below-treeline and above-treeline lakes ($r = 0.2$, $p = 0.018$, PERMANOVA). The terrestrial humic-like C1 component dominated the fluorescence composition, representing $64.6 \pm 30.3\%$ of the cDOM fluorescence in lakes below treeline; this share was significantly higher than that measured in the lakes above treeline ($42.9\% \pm 29.7\%$). Moreover, the proteinous C3 component was significantly lower in lakes below the treeline than in lakes above the treeline.

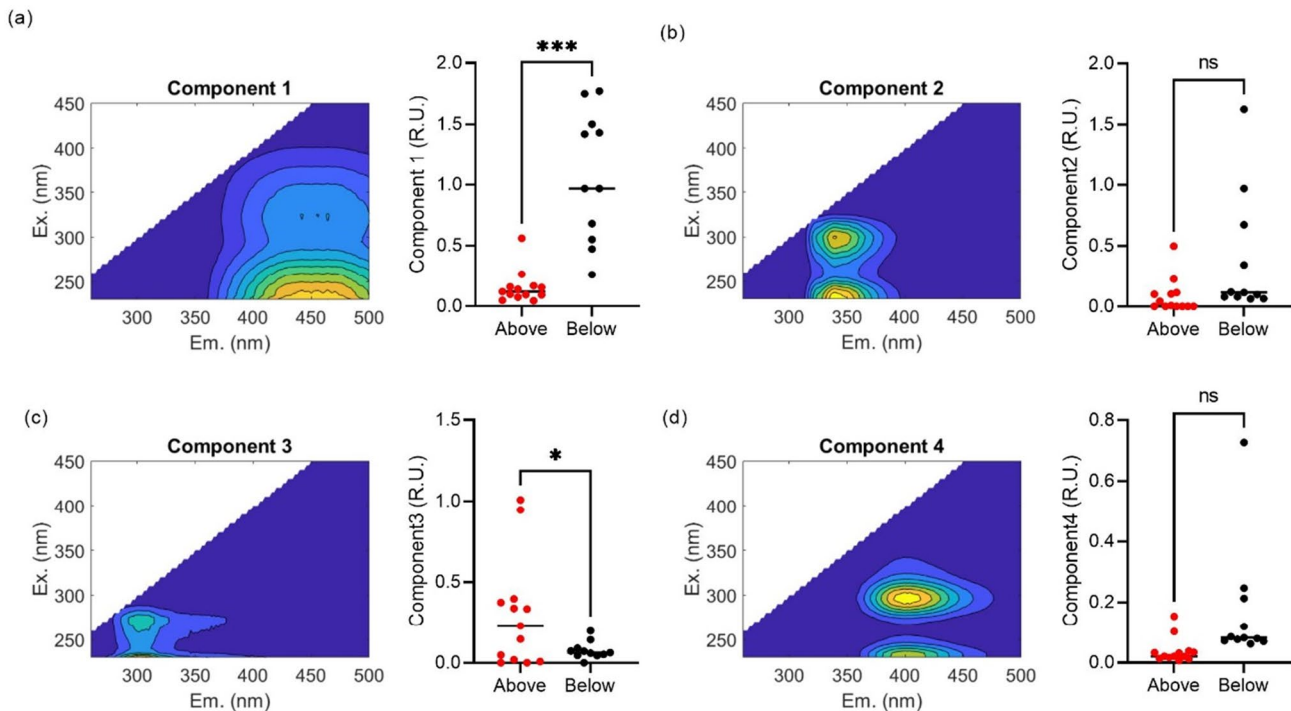


Fig. 3 The PARAFAC model output showing the fluorescence signatures of four fluorescent components of cDOM in the studied alpine lakes. The contour plots present the spectral shapes of excitation and emission. *** $p < 0.001$; * $p < 0.05$; ns, not significant

Bacterial Community Composition

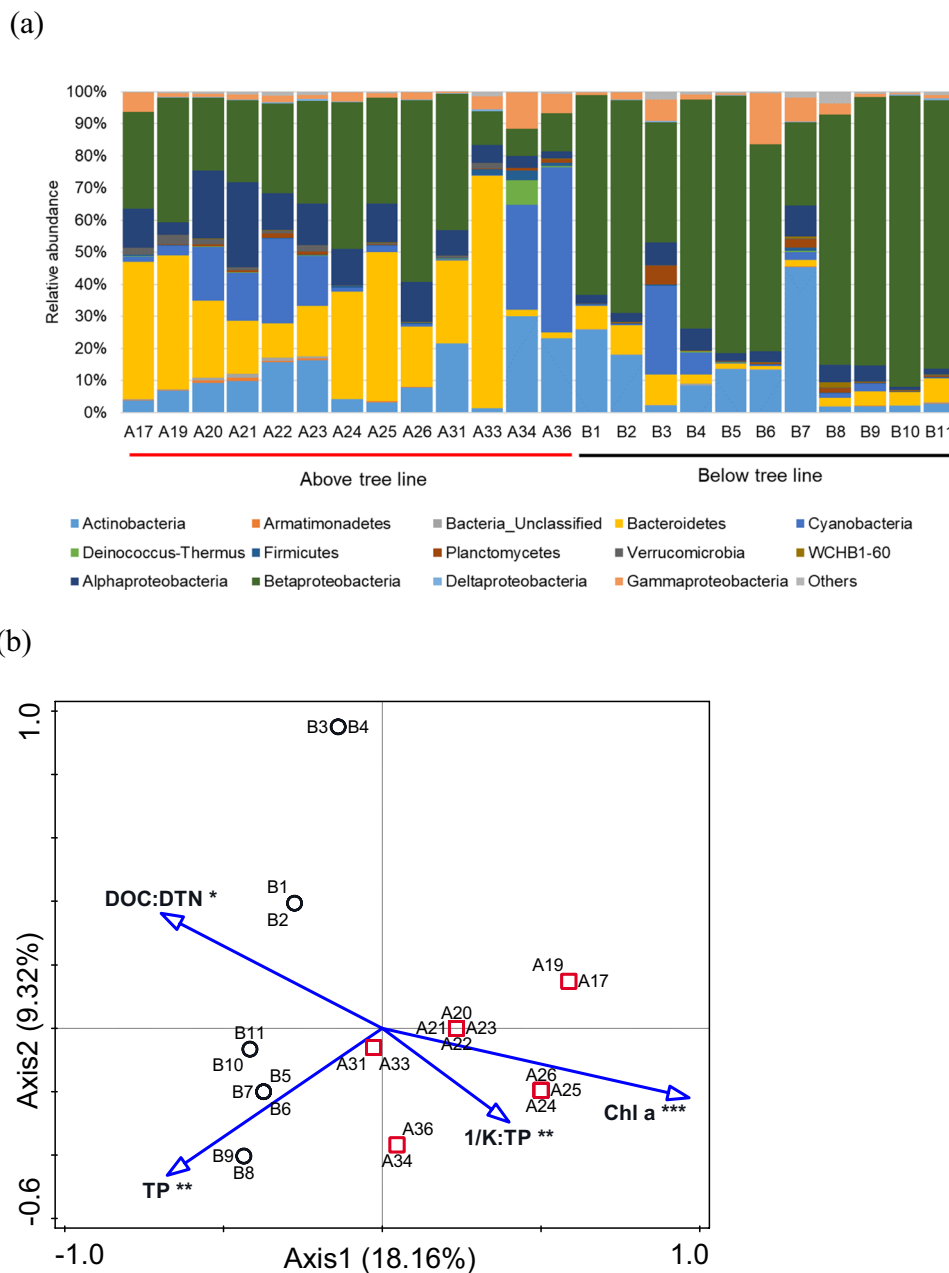
The total number of OTUs found in the above-treeline lakes were 2029 (474 ± 74 , $n = 13$), and that found in below-treeline lakes was 1805 (559 ± 194 , $n = 11$). The species richness of the lake microbes showed no significant difference between the below-treeline and above-treeline lakes (Table 1). The Bray–Curtis dissimilarities within each group (below or above treeline) were significantly smaller than those between the two groups (Fig. S3, Supporting Information).

In both regions, most OTUs were assigned to bacterial phyla, including Proteobacteria (1084 OTUs, 58.7% of all sequences), Bacteroidetes (424 OTUs, 16.9% of all sequences), Actinobacteria (139 OTUs, 12.0% of all sequences), Cyanobacteria (153 OTUs, 8.8% of all sequences). Moreover, Proteobacteria was major composed of Betaproteobacteria (117 OTUs, 47.1% of all sequences), Alphaproteobacteria (374 OTUs, 8.0% of all sequences) and Gammaproteobacteria (396 OTUs, 3.4% of all sequences, Fig. 4a). On average, all samples collected from lakes above treeline were dominated by Betaproteobacteria (mean: 29.7%), Bacteroidetes (mean: 27.1%), Cyanobacteria (mean: 12.9%), Actinobacteria (mean: 11.7%) and Alphaproteobacteria (mean: 11.0%). The bacterioplankton communities obtained from lakes

below treeline were primarily dominated by Betaproteobacteria (mean: 67.6%) and Actinobacteria (mean: 12.3%), whereas the average relative abundances of all the other phyla were below 5.0%.

The overall community compositions were significantly different between lakes above and below treeline ($r = 0.533$, $p = 0.001$). Among all the bacterial phyla, Betaproteobacteria was significantly enriched in samples from below-treeline lakes ($p < 0.001$), while Bacteroidetes ($p = 0.002$), Verrucomicrobia ($p = 0.002$), Alphaproteobacteria ($p = 0.002$) and Armatimonadetes ($p = 0.015$) were significantly higher in samples from above-treeline lakes (Fig. S4, Supporting Information). Forty-three genera out of all the detected genera differed significantly between the two regions, among which thirty-five genera were significantly more abundant in above-treeline lakes than in below-treeline lakes. The most abundant genus, *Poly-nucleobacter*, affiliated with Betaproteobacteria, was significantly enriched in the samples obtained from below-treeline lakes, with mean values of 28.9% in below-treeline samples and 4.6% in above-treeline samples ($p < 0.001$, Supporting Information Fig. S5). When investigating all the genera within the phylum Bacteroidetes, five were significantly abundant in samples from below-treeline lakes, such as *Fluviimonas*, *Ferruginibacter* and *Fluviivola*.

Fig. 4 Bacterial community composition in lakes located above and below treeline (a) and the redundancy analysis (RDA) ordination showing the correlations between the bacterial community compositions and the significant environmental factors (b). Black circles and red squares denote samples collected below and above treeline, respectively



Environmental Driving Factors of Bacterioplankton Communities

An initial RDA was performed between the pelagic OTU profiles and explanatory variables to determine whether environmental or spatial variables had an effect on the microbial assemblage composition. After stepwise forward selection, four environmental variables (Chl *a*, $p=0.001$; TP, $p=0.002$; $1/K:TP$, $p=0.002$; DOC:DTN, $p=0.039$; Fig. 4b, Table S2) showed significant correlations with the bacterial assemblage composition. Along the first axis of the RDA plot, $1/K:TP$ and Chl *a* were oriented in the same direction where the above-treeline samples clustered, but

DOC:DTN and TP were oriented in the opposite direction. In addition, the first two axes explained 18.36% and 9.12% of the total variations in the bacterioplankton community compositions of all the samples, respectively.

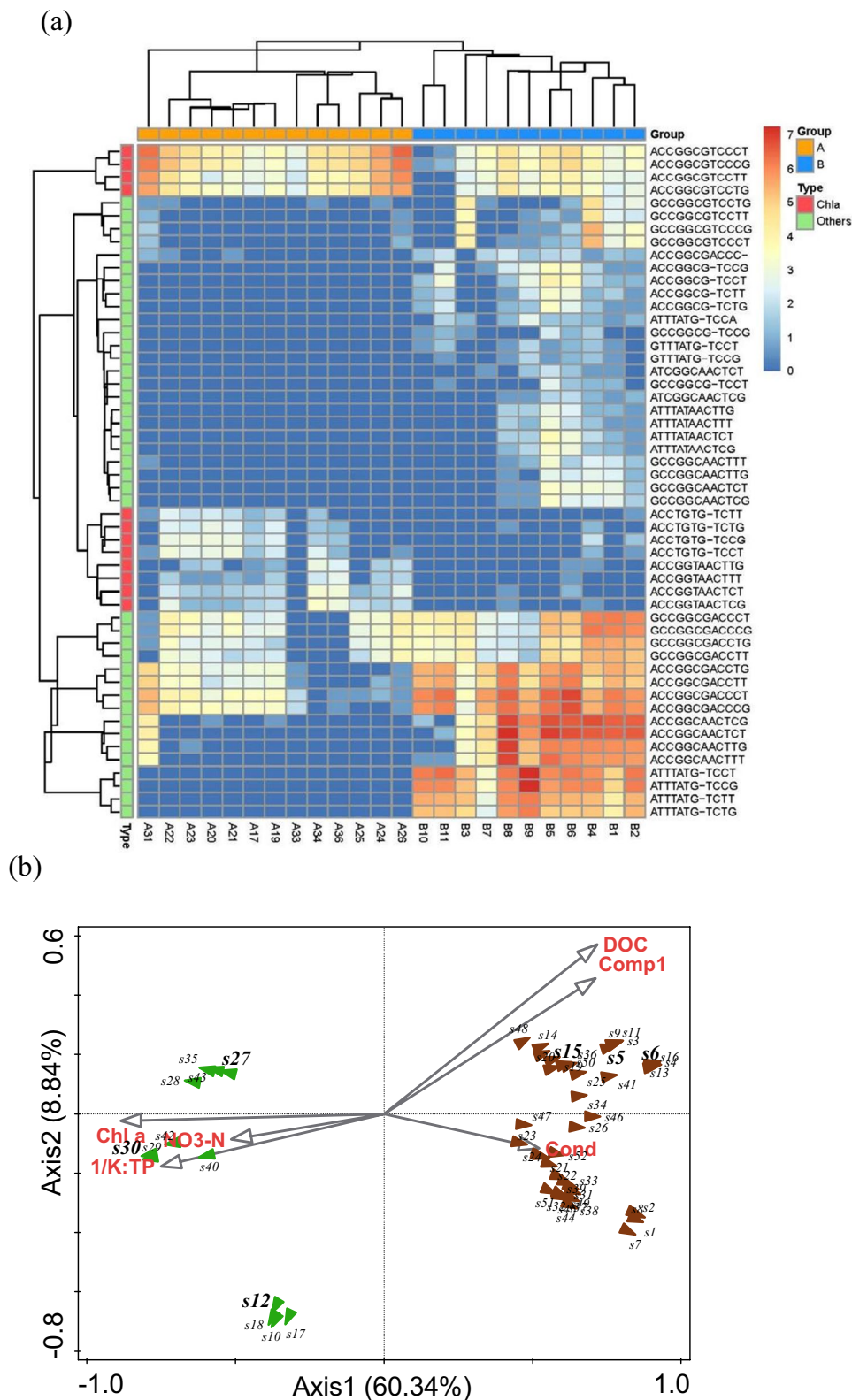
Micro-diversity and Niche Separation of Dominant *Polynucleobacter* OTUs

Three OTUs (OTU550, OTU1010 and OTU1160) were affiliated with the genus *Polynucleobacter*, among which OTU1010, affiliated with the PnecC cluster, was the most universally abundant, accounting for averages of 27.4% and 4.1% of reads in the lakes below and above treeline,

respectively. Fifty-two oligotypes were identified within OTU1010, and their distribution patterns were distinct between below-treeline and above-treeline lakes (Fig. 5a).

Six oligotypes found 100% identity sequences obtained from various freshwater all over the world (Table S3, supporting information). The oligotypes s5 and s15 were identical

Fig. 5 Oligotyping OTU1010 affiliated with the *Polynucleobacter* PncC clade in lakes located below and above treeline. Heatmap showing the abundances and distributions of the oligotypes (in the right column, $n = 52$) identified in each sample (a). Group A: above treeline (in orange), Group B: below treeline (in blue) and biplot showing the driving factors of different oligotypes (b). Red arrows represent the oligotypes detected in lakes located above the treeline, and green arrows represent those detected in lakes below the treeline. Numbers in bold faces were those six oligotypes having 100% identical sequences obtained from freshwater all over the world (detailed information was shown in supplementary table S3)



to type strains *P. duraquae* MWH-MoK4^T and *P. sinensis* MWH-HuW1^T, respectively. The other four oligotypes s6, s12, s27 and s30 were identical to some environmental *Poly-nucleobacter* 16S rRNA gene sequences. All the oligotypes were clearly divided into two groups: twelve were driven by 1/K:TP, Chl *a* concentrations and NO₃-N in the lakes above treeline, and the remaining 40 oligotypes were enriched in the lakes below treeline; these oligotypes were further roughly divided into two clusters, one correlating with the terrestrial humic-like C1 component and DOC concentrations, and the other correlating with conductivity of water (Fig. 5b, Table S4, supporting information).

Discussion

P Limitation for Bacteria in Above-Treeline Lakes and Light Limitation for Algae in Below-Treeline Lakes

The studied alpine lakes located below treeline were encircled by forests and meadows, and the terrestrial organic matter in these regions mainly consisted of humic substances; thus, the lake water appeared brown. In contrast, the lakes located above treeline were mainly surrounded by exposed heaps of rocks with extremely low concentrations of humic substances and cDOM. As a result, the underwater attenuation coefficients were low in these lakes, and the water was highly transparent.

Both of these alpine lake types are oligotrophic because the amounts of nutrients input from terrestrial sources are much lower than those in catchments where human activities have great impacts. Zhang et al. investigated 38 plateau lakes and found no eutrophic lakes at elevations higher than ~4000 m [13] and the N:P ratio is extremely high in most oligotrophic lakes. In this study, the mean N:P value measured in the above-treeline lakes was 66.6, and this value was 31.7 in the below-treeline lakes, both of which were higher than the Redfield value (~22) of the algal N:P ratio, particularly in the above-treeline lakes. Therefore, the P limitation appears to be more remarkable in these lakes. P limitation for bacteria under high light:TP conditions can be partly explained by high light energy and low nutrient utilization promoting carbon exudation rather than biomass production by phytoplankton. This explanation is based on the assumption that bacteria in these lakes mainly utilize autochthonous carbon such as algae. Although the carbon pools of the above-treeline lakes were mainly replenished by allochthonous carbon from glacial meltwater, the log(bacterial abundance) decreased with increasing Chl *a* concentrations (Fig. 2b, $R^2=0.62$). The relatively high phytoplankton biomasses (Chl *a* concentrations) and relatively low bacterial abundances measured in the above-treeline lakes suggested

that phytoplankton compete with bacteria for nutrients and obtain more P than bacteria do [2], thereby aggravating bacterial P limitation. Overall, the bacterial nutrient limitation in the above-treeline lakes with high light:nutrient (high 1/K:TP) conditions fit the light-to-nutrient hypothesis.

Sterner et al. proposed that under low light:TP conditions, planktonic bacteria are limited by C because phytoplankton have a high P utilization efficiency, promoting the production of phytoplankton biomass rather than the excretion of C [2]. Again, this explanation implies that bacteria mainly utilize algal carbon. However, in this work, in below-treeline lakes with low light:nutrient (low 1/K:TP) conditions, the log(bacterial abundance) had little correlation with the Chl *a* concentrations (Fig. 2b, $R^2=0.0005$). Notably, although the P limitation of bacteria was weakened under low light:TP conditions, bacteria did not appear to be subject to C limitation, but phytoplankton were subject to light limitation. In humic or turbid lakes, the influence of high cDOM concentrations or turbidity causes light to become a limiting factor for algae. The studied lakes located below treeline were rich in humic substances since they were surrounded by thick pinewood and evergreen broad-leaf forests, thereby presenting dark-brown colours. A high cDOM concentration results in rapid light attenuation in water. Consequently, weak light conditions limit the growth of algae, leading to low Chl *a* concentrations (Fig. 1c), and the growth of planktonic bacteria is strongly supported by allochthonous carbon. In the absence of C limitation and without significant P limitation, bacteria are likely to compete with algae for nutrients. Overall, the ecosystem processes in below-treeline lakes cannot be predicted using the light-to-nutrient hypothesis.

The traditional view holds that heterotrophic bacterioplankton greatly depend on the organic matter produced by phytoplankton, and the growth of phytoplankton is limited by light and nutrients such as N and P. The relationship between bacterial abundance and phytoplankton abundance in waters with low humic substance contents conforms to the classic interpretation described above. However, in some oligotrophic lakes, the C:P ratio of bacteria is tenfold lower than that of phytoplankton, and when the organic carbon supply is sufficient, heterotrophic bacterioplankton are able to compete with algae for limited inorganic nutrients [37]. This is most common in humic lakes located below treeline with high C:N (Fig. 2d) or C:P ratios. For example, the correlation between the bacterial abundance and chlorophyll concentration (a surrogate of algal abundance) was found to be weaker than that between bacteria and TP, reflecting the competition for P between bacteria and algae [38]. When organic carbon is abundant and/or the P concentration is low, heterotrophic bacteria are likely to have an advantage over algae when competing for P [38]. In general, we believe that this is the first study to verify the applicability of the light-nutrient

hypothesis in alpine lake ecosystems, and the nutrient limitations of bacterioplankton showed different scenarios in above-treeline and below-treeline lakes.

Bacterial Community Composition Was Sensitive to Allochthonous and Autochthonous Carbon

The effect of the light:P ratio on a bacterial community is mainly reflected by the amounts and compositions of organic carbon and phosphorus. In addition to potential P limitations in lakes located above treeline, light limitation affecting algae growth and organic carbon photodegradation in below-treeline lakes impact the organic carbon composition, thereby affecting the bacterial community distribution. The bacterioplankton communities demonstrated clear separation between lakes located below and above treeline. Furthermore, strong evidence was obtained that cryptic diversity in *Polynucleobacter* species is crucial when interpreting diversity studies on freshwater bacterioplankton conducted based on ribosomal sequences.

Polynucleobacter is a globally abundant freshwater bacteria, and its PncC cluster is a particularly interesting taxon used to study diversification in freshwater [39] due to its cosmopolitan distribution [40, 41] and high global abundance [42]. Its ecological success has been shown to be the result of diversification rather than a generalist adaptation, as lineages within the PncC cluster reveal distinct ecological characteristics [40, 43, 44]. Hahn et al. discovered that the PncC cluster was able to dwell in habitats covering a broad pH range, further emphasizing the differences among habitat-specific adaptations [45]. Until now, no field evidence was available for the carbon source spectrum of this diversified cluster. In this study, we found clear habitat-specific adaptations in lakes located below and above treeline and in the substrate preference within the same OTU. A small cluster including 12 oligotypes was directed towards the phytoplankton biomass index (Chl *a* concentration); this cluster probably relied on the autochthonous carbon produced by phytoplankton as its major organic carbon source. Alga-released organic matter is composed of a variety of low-molecular-weight to high-molecular-weight compounds predominantly comprising carbohydrates, nitrogenous substrates, lipids and organic acids [46]. The addition of extracellular and biomass-derived organic compounds initiated the growth of the *Polynucleobacter* PncB cluster [47, 48]. On the other hand, more diverse oligotypes were identified in the lakes located below treeline; these oligotypes might have adapted to the abundant structures of terrestrial carbon. Experiments have indicated that these bacteria live as chemorganotrophs by mainly utilizing low-molecular-weight substrates derived from the photooxidation of humic substances [49].

Implications for Bacterial Nutrient Limitation in High-Elevation and Polar Lakes

With climate warming, the global area of glaciers has decreased by ~17% in the last 30 years [50]. The proportion of glacier retreat on the Tibetan Plateau reached 95% ($n=116$) from 1990 to 2005 [51]. Future changes in glacial runoff will impact the bioavailability of organic carbon (OC) in downstream ecosystems. It has been reported that the bioavailability of DOC in glacial meltwater is 2–5 times higher than that in forested and wetland streams [52]. Therefore, it can be expected that the input of cryosphere-derived OC will increase in above-treeline lakes, subsidizing the carbon source of bacteria in these lakes.

In addition, the rapid development of industry and agriculture resulted in the nitrogen and phosphorus deposition rates doubling in Asia during the past 40 years [53]. Climate warming together with enhanced nutrient loading may have two consequences. One involves the rapid growth of algae in lakes and bacteria that do not lack nutrients. At present, a few alpine lakes have shown moderate eutrophication [54]. The other possible consequence is the rapid growth of terrestrial plants and the upward shift of treelines; under these circumstances, a catchment environment above treeline may gradually become more like the environment below treeline. A meta-analysis indicated that global treelines shifted upward during the last century at 52% of sites [55]. As a possible result, the presence of terrestrial humic substances will decrease the underwater light intensity and cause light limitation for algae. If the light:TP ratio decreases and the P limitation for bacteria further weakens in alpine lakes, bacteria will compete with algae. The conditions seem to be moving towards this scenario in below-treeline lakes.

However, lake ecosystems are complex and are affected by many factors other than climatic and environmental changes. We should also consider that different lakes have different topographical and hydrological characteristics and that predation has an extremely important effect on bacterial and algal community structures and their competitive relationships. Consequently, predicting how climatic and environmental changes in cryosphere ecosystems influence bacterial nutrient limitations and community structures remains a challenge. In the future, further studies of bacterial nutrient limitation changes and the driving forces that influence these changes will be of great significance for the stability and biodiversity of high-elevation and high-latitude aquatic ecosystems.

Conclusions

In this study, we demonstrated that the bacteria in above-treeline lakes are limited by P; however, the bacteria in below-treeline lakes are not limited by carbon, but the

algae in these lakes are limited by light due to the fast light attenuation by high concentrations of humic substances. The bacterioplankton communities demonstrated clear variation between the lakes located below and above treeline. Especially, *Polynucleobacter* OTU1010 could be subdivided into 52 oligotypes which had higher micro-diversity in the below-treeline lakes than the above-treeline lakes. The niche separations within a single OTU were demonstrated as versatile response to light-to-nutrient ratio and carbon sources. In conclusion, the light:P ratio and the composition and structure of organic matter have important implications for bacterioplankton nutrient limitations affecting their assemblage compositions in high-elevation lakes.

Supplementary Information The online version contains supplementary material available at <https://doi.org/10.1007/s00248-021-01834-4>.

Acknowledgements We would like to acknowledge W. Zhen, X. F. Zhao and J. L. Yu for field assistance.

Author Contribution Y.S. did the field sampling, physiochemical data analysis and wrote the draft manuscript. Y.D. did the cDOM measurement and data interpretation. P.X. did the microbial data analysis and modified the manuscript.

Funding National Natural Science Foundation of China (31971475, 31722008, 31670461) supported this publication.

Data Availability All bacterial 16S rRNA gene sequence data produced during the study were deposited in the NCBI Sequence Read Archive database under Bioproject PRJNA637707 via the accession numbers SRX8488122–SRX8488157.

Declarations

Conflict of Interest The authors declare no competing interests.

References

- Smol JP (2009) Pollution of lakes and rivers: a paleoenvironmental perspective. John Wiley & Sons
- Sterner RW, Elser JJ, Fee EJ, Guildford SJ et al (1997) The light : nutrient ratio in lakes: the balance of energy and material affects ecosystem structure and process. *Am Naturalist* 150:663–684. <https://doi.org/10.1086/286088>
- Obernosterer I, Herndl GJ (1995) Phytoplankton extracellular release and bacterial growth: dependence on the inorganic N : P ratio. *Mar Ecol Prog Ser* 116:247–257. <https://doi.org/10.3354/meps116247>
- Chrzanowski TH, Grover JP (2001) The light : nutrient ratio in lakes: a test of hypothesized trends in bacterial nutrient limitation. *Ecol Lett* 4:453–457. <https://doi.org/10.1046/j.1461-0248.2001.00244.x>
- Cole JJ, Caraco NF, Kling GW et al (1994) Carbon dioxide supersaturation in the surface waters of lakes. *Science* 265:1568–1570. <https://doi.org/10.1002/lob.10098>
- Jansson M, Bergström AK, Blomqvist P et al (1999) Impact of allochthonous organic carbon on microbial food web carbon dynamics and structure in Lake Örrträsket. *Arch Hydrobiol* 144:409–428
- Guillemette F, Bianchi TS, Spencer RG (2017) Old before your time: ancient carbon incorporation in contemporary aquatic food-webs. *Limnol Oceanogr* 62:1682–1700. <https://doi.org/10.1002/lno.10525>
- Wookey PA, Aerts R, Bardgett RD et al (2009) Ecosystem feedbacks and cascade processes: understanding their role in the responses of Arctic and alpine ecosystems to environmental change. *Glob Change Biol* 15:1153–1172. <https://doi.org/10.1111/j.1365-2486.2008.01801.x>
- Musselman RC, Slauson WL (2004) Water chemistry of high elevation Colorado wilderness lakes. *Biogeochemistry* 71:387–414. <https://doi.org/10.1007/s10533-004-0369-6>
- Elser JJ, Andersen T, Baron JS et al (2009) Shifts in lake N: P stoichiometry and nutrient limitation driven by atmospheric nitrogen deposition. *Science* 326:835–837. <https://doi.org/10.1126/science.1176199>
- Bobink R, Hicks K, Galloway J et al (2010) Global assessment of nitrogen deposition effects on terrestrial plant diversity: a synthesis. *Ecol Appl* 20:30–59. <https://doi.org/10.1890/08-1140.1>
- Su YL, Chen FZ, Liu ZW (2015) Comparison of optical properties of chromophoric dissolved organic matter (CDOM) in alpine lakes above or below the tree line: insights into sources of CDOM. *Photochem Photobiol Sci* 14:1047–1062. <https://doi.org/10.1039/c4pp00478g>
- Zhang YL, Zhang EL, Yin Y et al (2010) Characteristics and sources of chromophoric dissolved organic matter in lakes of the Yungui Plateau, China, differing in trophic state and altitude. *Limnol Oceanogr* 55:2645–2659. <https://doi.org/10.4319/lo.2010.55.6.2645>
- McKnight DM, Boyer EW, Westerhoff PK et al (2001) Spectrofluorometric characterization of dissolved organic matter for indication of precursor organic material and aromaticity. *Limnol Oceanogr* 46:38–48. <https://doi.org/10.4319/lo.2001.46.1.0038>
- Stedmon CA, Bro R (2008) Characterizing dissolved organic matter fluorescence with parallel factor analysis: a tutorial. *Limnol Oceanogr Methods* 6:1–6. <https://doi.org/10.4319/lom.2008.6.572>
- Cory RM, McKnight DM (2005) Fluorescence spectroscopy reveals ubiquitous presence of oxidized and reduced quinones in dissolved organic matter. *Environ Sci Technol* 39:8142–8149. <https://doi.org/10.1021/es0506962>
- Porter KG, Feig YS (1980) The use of DAPI for identification and enumeration of bacteria and blue-green algae. *Limnol Oceanogr* 25:943–948
- Caporaso JG, Lauber CL, Walters WA et al (2012) Ultra-high-throughput microbial community analysis on the Illumina HiSeq and MiSeq platforms. *ISME J* 6:1621–1624. <https://doi.org/10.1038/ismej.2012.8>
- Bolger AM, Lohse M, Usadel B (2014) Trimmomatic: a flexible trimmer for Illumina sequence data. *Bioinformatics* 30:2114–2120. <https://doi.org/10.1093/bioinformatics/btu170>
- Caporaso JG, Kuczynski J, Stombaugh J et al (2010) QIIME allows analysis of high-throughput community sequencing data. *Nat methods* 7:335–336. <https://doi.org/10.1038/nmeth.f.303>
- Edgar RC, Haas BJ, Clemente JC et al (2011) UCHIME improves sensitivity and speed of chimera detection. *Bioinformatics* 27:2194–2200. <https://doi.org/10.1093/bioinformatics/btr381>
- Edgar RC (2010) Search and clustering orders of magnitude faster than BLAST. *Bioinformatics* 26:2460–2461. <https://doi.org/10.1093/bioinformatics/btq461>
- Price MN, Dehal PS, Arkin AP (2010) FastTree 2—approximately maximum-likelihood trees for large alignments. *PLoS ONE* 5:e9490. <https://doi.org/10.1371/journal.pone.0009490>
- Quast C, Pruesse E, Yilmaz P et al (2013) The SILVA ribosomal RNA gene database project: improved data processing and

- web-based tools. *Nucleic Acids Res* 41:D590–D596. <https://doi.org/10.1093/nar/gks1219>
25. Wang Q, Garrity GM, Tiedje JM et al (2007) Naïve Bayesian classifier for rapid assignment of rRNA sequences into the new bacterial taxonomy. *Appl Environ Microbiol* 73:5261–5267. <https://doi.org/10.1128/AEM.00062-07>
 26. Eren AM, L. Maignien WJ, Sul LG, et al (2013) Oligotyping: differentiating between closely related microbial taxa using 16S rRNA gene data. *Methods Ecol Evol* 4:1111–1119. <https://doi.org/10.1111/2041-210X.12114>
 27. Parks DH, Tyson GW, Hugenholtz P et al (2014) STAMP: statistical analysis of taxonomic and functional profiles. *Bioinformatics* 30:3123–3124. <https://doi.org/10.1093/bioinformatics/btu494>
 28. Ter Braak CJF, Šmilauer P (2012) Canoco reference manual and user's guide: software for ordination, version 5.0. Microcomputer Power, Ithaca, USA
 29. Kalff J (2002) Limnology: inland water ecosystems. Prentice Hall, Upper Saddle River, New Jersey
 30. Coble PG (1996) Characterization of marine and terrestrial DOM in seawater using excitation-emission matrix spectroscopy. *Mar Chem* 51:325–346. [https://doi.org/10.1016/0304-4203\(95\)00062-3](https://doi.org/10.1016/0304-4203(95)00062-3)
 31. Walker SA, Amon RMW, Stedmon C et al (2009) The use of PARAFAC modeling to trace terrestrial dissolved organic matter and fingerprint water masses in coastal Canadian Arctic surface waters. *J Geophys Res Biogeosci* 114 (G4). <https://doi.org/10.1029/2009JG000990>
 32. Guéguen C, Cuss CW, Cassels CJ et al (2014) Absorption and fluorescence of dissolved organic matter in the waters of the Canadian Arctic Archipelago, Baffin Bay, and the Labrador Sea. *J Geophys Res Oceans* 119:2034–2047. <https://doi.org/10.1002/2013JC009173>
 33. Chen M, Kim SH, Jung HJ et al (2017) Dynamics of dissolved organic matter in riverine sediments affected by weir impoundments: production, benthic flux, and environmental implications. *Water Res* 121:150–161. <https://doi.org/10.1016/j.watres.2017.05.022>
 34. Stedmon CA, Thomas DN, Granskog M et al (2007) Characteristics of dissolved organic matter in Baltic coastal sea ice: allochthonous or autochthonous origins? *Environ Sci Technol* 41:7273–7279. <https://doi.org/10.1021/es071210f>
 35. Yamashita Y, Scinto LJ, Maie N et al (2010) Dissolved organic matter characteristics across a subtropical wetland's landscape: application of optical properties in the assessment of environmental dynamics. *Ecosystems* 13:1006–1019. <https://doi.org/10.1007/s10021-010-9370-1>
 36. Yamashita Y, Boyer JN, Jaffé R (2013) Evaluating the distribution of terrestrial dissolved organic matter in a complex coastal ecosystem using fluorescence spectroscopy. *Cont Shelf Res* 66:136–144. <https://doi.org/10.1016/j.csr.2013.06.010>
 37. Fagerbakke KM, Haldal M, Norland S (1996) Content of carbon, nitrogen, oxygen, sulfur and phosphorus in native aquatic and cultured bacteria. *Aquat Microb Ecology* 10:15–27. <https://doi.org/10.3354/ame010015>
 38. Currie DL (1990) Large-scale variability and interactions among phytoplankton, bacterioplankton and phosphorus. *Limnol Oceanogr* 35:1437–1455. <https://doi.org/10.4319/lo.1990.35.7.1437>
 39. Hahn MW (2003) Isolation of strains belonging to the cosmopolitan *Polynucleobacter necessarius* cluster from freshwater habitats located in three climatic zones. *Appl Environ Microbiol* 69:5248–5254. <https://doi.org/10.1128/AEM.69.9.5248-5254.2003>
 40. Hahn MW, Koll U, Jezberova J et al (2015) Global phylogeography of pelagic *Polynucleobacter* bacteria: restricted geographic distribution of subgroups, isolation by distance and influence of climate. *Environ Microbiol* 17:829–840. <https://doi.org/10.1111/1462-2920.12532>
 41. Hahn MW, Huemer A, Pitt A et al (2021) Opening a next-generation black box: ecological trends for hundreds of species-like taxa uncovered within a single bacterial >99% 16S rRNA operational taxonomic unit. *Mol Ecol Resour*. <https://doi.org/10.1111/1755-0998.13444>
 42. Jezberová J, Jezbera J, Brandt U et al (2010) Ubiquity of *Polynucleobacter necessarius* ssp. *asymbioticus* in lentic freshwater habitats of a heterogeneous 2000 km area. *Environ Microbiol* 12:658–669. <https://doi.org/10.1111/j.1462-2920.2009.02106.x>
 43. Jezbera J, Jezberova J, Brandt U et al (2011) Ubiquity of *Polynucleobacter necessarius* subspecies *asymbioticus* results from ecological diversification. *Environ Microbiol* 13:922–931. <https://doi.org/10.1111/j.1462-2920.2010.02396.x>
 44. Jezbera J, Jezberova J, Koll U et al (2012) Contrasting trends in distribution of four major planktonic betaproteobacterial groups along a pH gradient of epilimnia of 72 freshwater habitats. *FEMS Microbiol Ecol* 81:467–479. <https://doi.org/10.1111/j.1574-6941.2012.01372.x>
 45. Hahn MW, Jezberova J, Koll U et al (2016) Complete ecological isolation and cryptic diversity in *Polynucleobacter* bacteria not resolved by 16S rRNA gene sequences. *ISME J* 10:1642–1655. <https://doi.org/10.1038/ismej.2015.237>
 46. Sundh I (1992) Biochemical-composition of dissolved organic-carbon derived from phytoplankton and used by heterotrophic bacteria. *Appl Environ Microbiol* 58:2938–2947. [https://doi.org/10.1016/0378-1097\(92\)90407-F](https://doi.org/10.1016/0378-1097(92)90407-F)
 47. Horňák K, Kasalický V, Šimek K et al (2017) Strain-specific consumption and transformation of alga-derived dissolved organic matter by members of the *Limnohabitans-C* and *Polynucleobacter-B* clusters of Betaproteobacteria. *Environ Microbiol* 19:4519–4535. <https://doi.org/10.1111/1462-2920.13900>
 48. Nuy JK, Hoetzing M, Hahn MW et al (2020) Ecological differentiation in two major freshwater bacterial taxa along environmental gradients. *Front Microbiol* 11:154. <https://doi.org/10.3389/fmicb.2020.00154>
 49. Hahn MW, Scheuerl T, Jezberova J et al (2012) The passive yet successful way of planktonic life: genomic and experimental analysis of the ecology of a free-living *Polynucleobacter* population. *PLoS ONE* 7:e32772. <https://doi.org/10.1371/journal.pone.0032772>
 50. Qiu J (2010) Measuring the meltdown. *Nature* 468:141–142. <https://doi.org/10.1038/468141a>
 51. Li ZG (2014) Glacier and lake changes across the Tibetan plateau during the past 50 years of climate change. *J Resour Ecol* 5:123–131. <https://doi.org/10.5814/j.issn.1674-764x.2014.02.004>
 52. Hood E, Fellman J, Spencer RGM et al (2009) Glaciers as a source of ancient and labile organic matter to the marine environment. *Nature* 462:1044–1047. <https://doi.org/10.1038/nature08580>
 53. Zheng X, Fu C, Xu X et al (2002) The Asian nitrogen cycle case study. *Ambio* 31:79–87. <https://doi.org/10.1579/0044-7447-31.2.79>
 54. Bergström A, Jansson M (2006) Atmospheric nitrogen deposition has caused nitrogen enrichment and eutrophication of lakes in the northern hemisphere. *Glob Change Biol* 12:635–643. <https://doi.org/10.1111/j.1365-2486.2006.01129.x>
 55. Harsch MA, Hulme PE, McGlone MS et al (2009) Are treelines advancing? A global meta-analysis of treeline response to climate warming. *Ecol Lett* 12:1040–1049. <https://doi.org/10.1111/j.1461-0248.2009.01355.x>